

Constraining Effective Field Theories for dark matter candidates annihilating into gamma-ray lines with CTAO

Lucia Angel^{a,b,c}, Debasish Borah^d, Jacinto P. Neto^{a,b,e,f},
Farinaldo S. Queiroz^{a,b,c,g}, Vitor de Souza^h

^aDepartamento de Física, Universidade Federal do Rio Grande do Norte, 59078-970, Natal, RN, Brasil

^bInternational Institute of Physics, Federal University of Rio Grande do Norte, Campus Universitário, Lagoa Nova, Natal-RN 59078-970, Brazil

^cMillennium Institute for Subatomic Physics at the High-Energy Frontier (SAPHIR) of ANID, Fernández Concha 700, Santiago, Chile

^dDepartment of Physics, Indian Institute of Technology, Guwahati, Assam 781039, India

^eDipartimento di Scienze Matematiche e Informatiche, Scienze Fisiche e Scienze della Terra, Università degli Studi di Messina, Viale Ferdinando Stagno d'Alcontres 31, I-98166 Messina, Italy

^fMax Planck Institut für Kernphysik, Saupfercheckweg 1, D-69117 Heidelberg, Germany

^gUniversidad de La Serena, Casilla 554, La Serena, Chile

^hInstituto de Física de São Carlos, Universidade de São Paulo, Av. Trabalhador São Carlense 400, São Carlos-SP, 13566-590, Brazil

E-mail: lucia.correa.717@ufrn.edu.br, dborah@iitg.ac.in,
jacinto.neto.100@ufrn.edu.br, farinaldo.queiroz@ufrn.br, vitor@ifsc.usp.br

Abstract. Gamma-ray lines constitute a smoking gun signature for annihilating dark matter particles. Imaging Atmospheric Cherenkov Telescopes and satellites have searched for such signals but null results have been reported thus far. We take advantage of the expected gamma-ray flux sensitivity of the Cherenkov Telescope Array Observatory (CTAO) toward the direction of the Galactic Centre and Dwarf Galaxies and its exquisite energy resolution to derive upper limits on fermionic and scalar dark matter annihilations into gamma-ray lines. We consider the lowest-order effective operators for scalar and fermion dark matter, and derive limits on the energy scale using the recent CTAO projected sensitivity. Putting our findings into perspective with existing limits from direct and indirect detection experiments, we conclude that CTAO will either play a complementary role or be a discovery channel for dark matter signals.

Contents

1	Introduction	1
2	Signal from the Dark Side	3
3	Dark Matter Effective Field Theory	4
4	Averaged Annihilation Cross-Sections	5
5	Existing Limits	7
5.1	Continuum gamma-ray bounds	7
5.2	Direct detection	9
6	Results	10
7	Conclusions	12

1 Introduction

The nature of dark matter (DM), despite numerous cosmological and astronomical observations, remains elusive [1]. Various experimental efforts aim to detect non-gravitational interactions of dark matter, including direct detection through nuclear scattering [2, 3] and production in particle accelerators [4, 5]. An exciting approach involves identifying dark matter annihilation products into Standard Model (SM) particles [6–9], known in the literature as indirect dark matter detection. Among the possible annihilation products, gamma rays and neutrinos are excellent messengers as they are not deflected by magnetic fields, thus retaining directional information. Unlike charged particles, they travel largely unimpeded, allowing them to carry spectral and spatial information across the cosmos.

It is plausible that dark matter particles, which interact with the SM particles in the early Universe, continue to do so today, particularly in regions with high dark matter density such as the Galactic Centre (GC) and Dwarf Spheroidal Galaxies (dSphs). The GC has the largest J -factors, making it the brightest dark matter source in the sky and, for this reason, a typical target for dark matter signals. On the other hand, dSphs, which are dominated by dark matter with little interstellar gas, do not have as large a J -factor, but are subject to relatively fewer background sources [10–12]. In other words, the GC often gives rise to the strongest limits.

These annihilations can generate a continuous gamma-ray emission with a bump-like feature and are subject to challenging astrophysical background sources [13–28]. However, the annihilation into photon pairs, resulting in monochromatic photons, provides a distinct signature due to the relative scarcity of similar astrophysical phenomena. Detection of such gamma-ray lines could directly point to the dark matter mass because the spectrum has a Gaussian-like shape centered at the dark matter mass. Gamma-ray observatories such as H.E.S.S and *Fermi* LAT have searched for gamma-ray line signatures from the Milky Way’s central region but found no excess signal, setting upper limits on the dark matter annihilation cross-section [6–8].

In models where the dark matter particle is thermally produced, we expect an annihilation cross-section around $\langle\sigma_{\text{ann}}v\rangle \sim 10^{-26} \text{ cm}^3 \text{ s}^{-1}$ [29]. Current gamma-ray telescopes are now probing this thermal cross-section in the 10 GeV to 100 GeV mass range for particular annihilation final states. Dark matter annihilations into fermions and gauge bosons produce generic spectra, but as the annihilation cross-section is typically orders of magnitude larger than that into

gamma-ray lines, they offer a better constraining power. Although, gamma-ray lines are loop-suppressed processes, with cross-section ranging from $10^{-28} \text{ cm}^3 \text{ s}^{-1}$ to $10^{-31} \text{ cm}^3 \text{ s}^{-1}$ depending on theoretical modeling, they do offer a more promising discovery channel.

We are commencing an era where the detection of positive gamma-ray line signals from TeV dark matter annihilation is within reach. The Cherenkov Telescope Array Observatory (CTAO) is under construction and will outperform the existing gamma-ray instruments. The energy resolution¹ is smaller than $\Delta E/E < 0.1$, and an effective area [30] nearly an order of magnitude larger than that of *Fermi* LAT for gamma-ray energies above 1 TeV make CTAO an excellent laboratory for probing dark matter annihilations and decays. When operating, CTAO shall be able to detect gamma rays from below 20 GeV to 300 TeV [30]. Therefore, CTAO will effectively probe Weakly Interacting Massive Particles (WIMPs) across three orders of magnitude in energy.

In this work, we are focused on gamma-ray lines, where energy resolution is the key. Box-shaped signals [31, 32] and other enhanced gamma-ray emission near the dark matter mass may mimic the effect of a gamma-ray line [33]. Hence, having a good energy resolution will allow us to discriminate dark matter signals from background sources and give insights into the underlying dark matter model behind the detected signal. The spatial morphology is key to separating a dark matter signal from a background source [10, 34]. Instead, gamma-ray lines offer more distinct signals hardly mimicked by astrophysical sources, see Fig. 1 below.

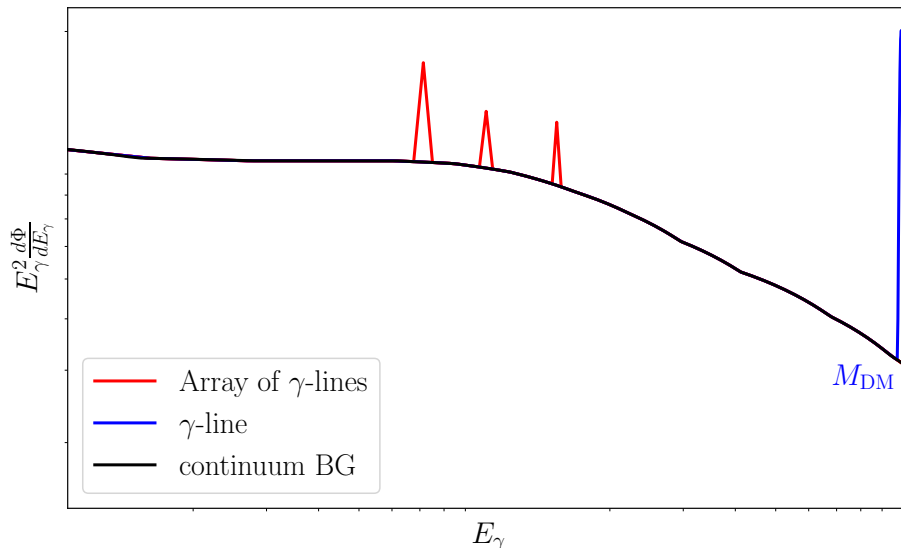


Figure 1: An illustration of how we expect to see gamma-ray lines from the differential flux. Either in a series of lines from a dark matter bound-state model (red) or a characteristic signal at the end of the spectrum from a model with a specific dark matter mass (blue) continuum emissions (black). Figure inspired by [35].

It is worth highlighting that the expected sensitivity we use to constrain the dark matter effective field theory (EFT) considered here is based on the so-called ‘Alpha’ configuration, which is the first-stage of CTAO construction [9, 36]. Furthermore, the CTAO will achieve better sensitivities than current Imaging Atmospheric Cherenkov Telescopes (IACT) generation instruments by a factor of 5 to 10 [37], resulting in an energy resolution of approximately $\Delta E/E \sim \mathcal{O}(0.1)$ TeV. For more details, the interested reader can look at Fig. 1 in [9]. Once

¹The energy resolution is quantified through the distribution of the relative energy error, $(E_R - E_T)/E_T$, commonly expressed as $\Delta E/E$, where E_R and E_T denote the reconstructed and true energies, respectively, of gamma-ray events observed with CTAO [30].

again, it shows how powerful and excellent such an instrument is for searching for exotic localized spectral features over many orders of magnitude in gamma-ray energies.

Our goal is to assess the CTAO sensitivity to gamma-ray lines arising from fermion and scalar dark matter stemming from the GC and dSphs. We describe them in terms of effective operators and determine the dark matter signal as a function of the effective energy scale. More importantly than simply showing the CTAO bounds, we put our findings into perspective by comparing them with direct detection experiments and continuum gamma-ray emission stemming from these operators. Therefore, our work advances in comparison to previous assessments of this nature [22, 38–45].

This paper is organized as follows: In Section 2, we briefly discuss the gamma-ray line from DM annihilation followed by listing the relevant EFT operators for DM annihilation into gamma-rays in Section 3; In Section 4, we calculate DM annihilation into two photons for both scalar and fermion DM considering dimension six and dimension five operators respectively; In Section 5 we discuss the existing bounds on such DM EFT operators from continuum gamma-ray emission and direct detection; Lastly, in Section 6 we present our results before drawing our conclusions in Section 7.

2 Signal from the Dark Side

We devote this section to introducing essential definitions related to the gamma-ray flux. The differential gamma-ray flux observed in a given solid angle element $d\Omega$ on the sky for the $X\bar{X} \rightarrow \gamma\gamma$ annihilation process, with photon energy $E = m_X$, is given by [11, 46]

$$\frac{d\Phi}{d\Omega dE} = \frac{r_\odot}{4\pi} \left(\frac{\rho_\odot}{2m_X} \right)^2 J_{\text{ann}}(\theta) \langle \sigma_{\text{ann}} v \rangle \frac{dN_\gamma}{dE} \quad (2.1)$$

where m_X is the mass of a generic dark matter particle X , which we consider not to be its own antiparticle, ρ_\odot is the dark matter energy density at the position, r_\odot , of the Solar System in the Milky Way, $\langle \sigma_{\text{ann}} v \rangle$ is the velocity averaged annihilation cross-section, with v standing for the dark matter relative velocity, and the annihilation J_{ann} -factor, integrated over the line-of-sight (l.o.s.), is defined as,

$$J_{\text{ann}}(\theta) = \int_{\text{l.o.s.}} \left(\frac{\rho(r)}{\rho_\odot} \right)^2 \frac{dl}{r_\odot}, \quad (2.2)$$

with $\rho(r)$ being the dark matter density profile, located at a distance l to the Earth and angle θ concerning the center of the dark matter halo, so that $r(l, \theta)$. Finally, the total gamma-ray energy spectrum per annihilation is,

$$\frac{dN_\gamma}{dE} = 2\delta(E - m_X), \quad (2.3)$$

where we get a factor of 2 since each annihilation produces two photons with energy equal to the dark matter particle mass.

It is important to note that Ω represents the solid angle in the sky and is used in the differential flux, while θ describes the observation direction relative to a point of interest (such as the center of a dark matter halo) and is used in calculating the J -factor. By considering both θ and Ω , we can accurately describe the spatial distribution of the gamma-ray flux from dark matter annihilation across the sky and understand how it varies based on the observation direction.

The predicted dark matter signal from the Galactic Centre is subject to large uncertainties from the astrophysical J -factor, as the dark matter density profile in the inner Galaxy is poorly constrained by observations. Guided by N-body simulations, the CTAO collaboration has adopted the Einasto profile as its benchmark (see Fig. 2) [9, 34], justifying our choice of adopting the same profile.

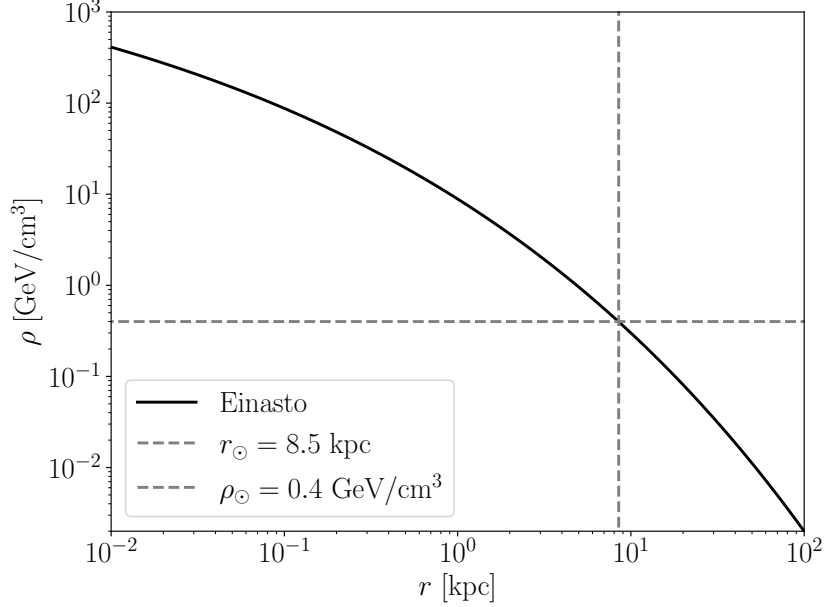


Figure 2: Einasto dark matter density profiles for the Galactic halo as a function of the distance to the Galactic Centre.

3 Dark Matter Effective Field Theory

We explore an EFT description of the dark matter annihilation into gamma-ray lines. This is a minimalistic approach as the DM phenomenology can be described with very few free parameters, namely, DM mass, cutoff scale, and the corresponding Wilson coefficients. Such EFT descriptions of DM have been studied extensively in the context of direct detection, indirect detection, as well as collider searches in several works [47–52], also summarised in a recent review [53]. In this present framework, we consider two possible DM candidates namely, a complex scalar S and a Dirac fermion χ which are singlets under the $SU(3)_c \otimes SU(2)_L \otimes U(1)_Y$ gauge symmetry of the SM. A separate symmetry ensures the stability of DM such that all effective operators involve DM bilinears only². We focus on effective operators of the lowest order because higher-order operators are relatively suppressed by higher powers of the effective energy scale Λ .

There are inherent advantages and limitations to the EFT approach. It is particularly applicable when the momentum transfer in a process is significantly lower than the mass of the mediator linking the dark and visible sectors. For dark matter annihilations, which are typically non-relativistic, the momentum transfer is of the order of the dark matter mass, making EFT a convenient method to evaluate such models. In Tables 1 and 2, we list the lowest-order effective operators that produce gamma-ray lines for both scalar and fermionic dark matter types, consistent with the chosen symmetries of our framework.

Our EFT framework includes the SM particles plus a dark matter component, X , which can be either a complex scalar or a Dirac fermion. If X is an antiparticle of itself, the results differ by a factor of two. As our goal is to study DM annihilation into photons, the EFT is formulated in terms of DM bilinears and $W_{\mu\nu}^a$, $B_{\mu\nu}$ representing the field strength tensors for the $SU(2)_L$ and $U(1)_Y$ groups, respectively³. The operators listed in Tables 1-2 are expressed in terms of these field strength tensors of gauge fields, which, after spontaneous electroweak

²We remain agnostic about the possible UV completions of such stabilising symmetry.

³A general field strength tensor is defined as $F_{\mu\nu}^a \equiv \partial_\mu F_\nu^a - \partial_\nu F_\mu^a + g f^{abc} F_\mu^b F_\nu^c$, where g is the coupling constant and f^{abc} are the structure constants for the symmetry group, with $f^{abc} = 0$ for Abelian theories.

symmetry breaking, relate to the mass eigenstates,

$$B_\mu = \cos \theta_W A_\mu - \sin \theta_W Z_\mu, \quad (3.1)$$

$$W_\mu^3 = \sin \theta_W A_\mu + \cos \theta_W Z_\mu, \quad (3.2)$$

where A_μ and Z_μ , are the neutral electroweak gauge bosons mass eigenstates, and θ_W is the Weinberg angle. Our analysis will focus exclusively on effective operators up to dimension six, as these encompass all potential leading-order annihilation channels into gamma-ray lines for fermion and scalar DM. This comprehensive list forms the basis of our study, delimiting the scope of these specific interactions.

Complex Scalar Dark Matter – Dimension 6 Operators		
S1	$\frac{1}{\Lambda_{S1}^2} SS^* B_{\mu\nu} B^{\mu\nu}$	$\gamma\gamma$
S2	$\frac{1}{\Lambda_{S2}^2} SS^* W_{\mu\nu}^a W^{a\mu\nu}$	$\gamma\gamma, \gamma Z$
S3	$\frac{1}{\Lambda_{S3}^2} SS^* B_{\mu\nu} \tilde{B}^{\mu\nu}$	$\gamma\gamma$
S4	$\frac{1}{\Lambda_{S4}^2} SS^* W_{\mu\nu}^a \tilde{W}^{a\mu\nu}$	$\gamma\gamma, \gamma Z$

Table 1: List of effective interactions for complex scalar dark matter and the type of line signals ($\gamma\gamma, \gamma Z$).

Dirac Fermion Dark Matter – Dimension 5 Operators		
F1	$\frac{1}{\Lambda_{F1}} \bar{\chi} \gamma^{\mu\nu} \chi B_{\mu\nu}$	$\gamma\gamma$
F2	$\frac{1}{\Lambda_{F2}} \bar{\chi} \gamma^{\mu\nu} \chi \tilde{B}_{\mu\nu}$	$\gamma\gamma, \gamma Z$

Table 2: List of effective interactions for Dirac fermion dark matter and the type of line signals ($\gamma\gamma, \gamma Z$). Note that $\gamma^{\mu\nu} = \frac{i}{2}[\gamma^\mu, \gamma^\nu]$.

With these operators at hand, our next step is to compute their averaged annihilation cross-section.

4 Averaged Annihilation Cross-Sections

The thermally averaged annihilation cross-section normalizes the gamma-ray flux resulting from dark matter annihilation, as can be seen in Eq.(4.1). In the non-relativistic limit, it can be approximated to be [54]

$$\langle \sigma_{\text{ann}} v \rangle \simeq \sigma_0 + \frac{1}{2} b v^2, \quad (4.1)$$

where $\sigma_s \equiv \sigma_0$ is the s-wave contribution that does not depend on the velocity and $\sigma_p \equiv b v^2/2$ is the velocity-dependent p-wave contribution. Such an expression translates the impact of the velocity dependence of the cross-section, as the dark matter velocity changes from freeze-out to the late-time Universe. We expect dark matter particles to be cold today, with radial velocity dispersion $v \sim \mathcal{O}(10^{-3})$ in the Galactic halo [55]. Thus, we can safely neglect the p-wave component and focus our reasoning on the s-wave term.

We assume p_1 and p_2 as the momenta of the incoming dark matter particles, p_3 and p_4 as the momenta of the outgoing particles. For concreteness, we take p_4 as the momentum for the Z boson for γZ final state. Hence, the differential cross-section is written,

$$\frac{d\sigma_0}{d\Omega} = \frac{E_3}{256\pi^2 E^3 v} |\overline{\mathcal{M}}|^2, \quad (4.2)$$

where $E = m_X + \mathcal{O}(v^2)$ is the energy of each dark matter particle, v is the dark matter velocity and $E_3 = |\vec{p}_3|$ is the energy of the outgoing photon. Moreover, $|\overline{\mathcal{M}}|^2$ is the amplitude \mathcal{M} squared

averaged over initial dark matter spins and summed over final state particle spins, which will be obtained below. Therefore, once we find $|\overline{\mathcal{M}}|^2$, we can immediately find the thermally averaged annihilation cross section, σ_0 , using Eq.(4.1) and Eq.(4.2).

The effective interactions between the scalar dark matter S and the neutral electroweak gauge bosons are shown in Tab. 1 via the S1–S4 operators. For S1 and S2 operators, involving the contraction of the strength tensors $B_{\mu\nu}B^{\mu\nu}$ and $W_{\mu\nu}^aW^{a\mu\nu}$, respectively, the amplitude for two final state photons is,

$$\mathcal{M}(SS^* \rightarrow \gamma\gamma) = 2Y [(p_3 \cdot p_4)(\varepsilon_3 \cdot \varepsilon_4) - (p_3 \cdot \varepsilon_4)(p_4 \cdot \varepsilon_3)], \quad \text{with} \quad Y \equiv \frac{\cos^2 \theta_W}{\Lambda}, \quad (4.3)$$

where $p_{3,4}$ are the outgoing momenta of the photons with respective polarization vectors $\varepsilon_{3,4}$. Summing over the spins, the amplitude squared reads,

$$\sum_{\varepsilon_e, \varepsilon_4} |\mathcal{M}(SS^* \rightarrow \gamma\gamma)|^2 = 4Y Y^\dagger \frac{s^2}{2} = \frac{2s^2 \cos^4 \theta_W}{\Lambda^4}, \quad (4.4)$$

where $s^2 = (p_3 + p_4)^2$. Considering the same operators but for a photon and a Z final state, the spin-averaged amplitude squared is,

$$\sum_{\varepsilon_e, \varepsilon_4} |\mathcal{M}(SS^* \rightarrow \gamma Z)|^2 = 4Y_1 Y_1^\dagger \frac{1}{2} (s - m_Z^2)^2 = \frac{2 \sin^2(2\theta_W)}{\Lambda^4} (s - m_Z^2)^2, \quad (4.5)$$

where $Y_1 = \sin(2\theta_W)/\Lambda$ and p_4 the Z boson momentum. Finally, we plug Eqs. (4.4) and (4.5) into Eq. (4.2), to obtain the average annihilation cross-sections for the S1 (S3) operator into $\gamma\gamma$ and γZ lines,

$$\langle \sigma(SS^* \rightarrow \gamma\gamma) v \rangle = \frac{\cos^4(\theta_W)}{\pi} \frac{m_S^2}{\Lambda_{S1}^4}, \quad (4.6)$$

$$\langle \sigma(SS^* \rightarrow \gamma Z) v \rangle = \frac{\sin^2(2\theta_W)}{\pi} \frac{m_S^2}{\Lambda_{S1}^4} \left(1 - \frac{m_Z^2}{4m_S^2}\right)^3, \quad (4.7)$$

and for the S2 (S4) operator,

$$\langle \sigma(SS^* \rightarrow \gamma\gamma) v \rangle = \frac{\sin^4(\theta_W)}{\pi} \frac{m_S^2}{\Lambda_{S2}^4}, \quad (4.8)$$

$$\langle \sigma(SS^* \rightarrow \gamma Z) v \rangle = \frac{\sin^2(2\theta_W)}{\pi} \frac{m_S^2}{\Lambda_{S2}^4} \left(1 - \frac{m_Z^2}{4m_S^2}\right)^3. \quad (4.9)$$

The same formalism is applied to the fermionic dark matter χ for F1 and F2 operators. However, we have to go to second-order perturbation theory to get the relevant contribution for $\gamma\gamma$ and γZ final states. In this case, the averaged annihilation cross-sections into both $\gamma\gamma$ and γZ final states are given by,

$$\langle \sigma(\chi\bar{\chi} \rightarrow \gamma\gamma) v \rangle = \frac{8}{\pi} \cos^4(\theta_W) \frac{m_\chi^2}{\Lambda_F^4}, \quad (4.10)$$

$$\langle \sigma(\chi\bar{\chi} \rightarrow \gamma Z) v \rangle = \frac{2}{\pi} \sin^2(2\theta_W) \frac{m_\chi^2}{\Lambda_F^4} \left(1 + \frac{m_Z^2}{4m_\chi^2}\right)^2 \left(1 - \frac{m_Z^2}{4m_\chi^2}\right). \quad (4.11)$$

Regardless of the astrophysical target, the scalar dark matter annihilation into $\gamma\gamma$ has a larger cross-section for the S1 (associated with $B_{\mu\nu}B^{\mu\nu}$) operator than the S2 (involving $W_{\mu\nu}^aW^{a\mu\nu}$) one due to the symmetry factor from the presence of identical particles in the final state. The γZ final state curves slope down as the dark matter mass decreases because the averaged annihilation

cross-section is proportional to $1 - m_Z^2/(4m_S^2)$, which is related to the energy resolution of the experiment as we will discuss below. Comparing the results from the $\gamma\gamma$ and γZ lines for S1 and S2 operators considering $m_S \gtrsim 100$ GeV, we note that for S1 they are very close, but for S2 operator the γZ lines correspond to larger cross-sections. Moreover, comparing Eqs. (4.9) and (4.11), we note that the fermion averaged annihilation cross-section is larger than the scalar one for the same DM mass. We assume $\Lambda_{F1} = \Lambda_{F2} = \Lambda_F$ throughout.

One should keep in mind that the γZ lines happen as long as $m_X > m_Z/2$, and the total thermally averaged annihilation cross-section for a dark matter particle $X = S, \chi$ must consider both $\gamma\gamma$ and γZ lines,

$$\langle \sigma_{\text{ann}} v \rangle = \langle \sigma(XX \rightarrow \gamma\gamma) v \rangle + \langle \sigma(XX \rightarrow \gamma Z) v \rangle \Theta \left[\frac{\Delta E}{E} - \frac{m_Z^2}{4m_X^2} \right], \quad (4.12)$$

where Θ is the Heaviside step function and $\Delta E/E$ is the energy resolution of the instrument, which is energy-dependent. We highlight there is no infinite-energy-resolution telescope. The telescope's energy dispersion, or finite energy resolution, is related to its response function. The expected energy resolution for CTAO is $\Delta E/E \sim 10\%$ between 1 TeV and 100 TeV [9]. The final state photons have different energies depending on the number of lines, say,

$$E_{\gamma\gamma} = m_X, \quad (4.13)$$

$$E_{\gamma Z} = m_X - \frac{m_Z^2}{4m_X}. \quad (4.14)$$

We can check in Eq. (4.12) via the Heaviside function, that the detector will not be able to distinguish between the two possible final states if the relative difference between their energies is up to the energy resolution of the instrument, i.e. $(E_{\gamma\gamma} - E_{\gamma Z})/E_{\gamma\gamma} \leq \Delta E/E$. Therefore, we must insert the CTAO energy resolution into Eq. (4.12) to derive the correct constraints.

That said, in the next section, we present the existing bounds on the effective operators based on continuous gamma-ray emission and direct detection.

5 Existing Limits

Although we focus on placing bounds from gamma-ray lines, the effective operators in this work also yield a continuum gamma-ray spectrum and DM-nucleon recoil at direct detection experiments. Hence, it is important to put our findings into perspective with direct detection, and the natural continuum gamma-ray spectrum whenever present to assess the role of the CTAO regarding probing gamma-ray lines signals from dark matter annihilation.

5.1 Continuum gamma-ray bounds

We present the bounds from H.E.S.S. and expected limits from CTAO for dark matter annihilation into charged final states, such as W^+W^- and $\tau^+\tau^-$, in the GC, considering the Einasto density profile [34, 56]. For the continuum spectrum, the H.E.S.S. dataset was collected over 6 years, and after data quality selection, the analysis used a total of 546 hours of live observation time. The CTAO expected limits assume a total observation time of 525 hours. The Fermi-LAT collaboration has adopted a different density profile, namely, Navarro-Frenk-White (NFW) and generalized NFW (gNFW) [57]. Thus, we decided to keep only the H.E.S.S. bound to make a fair comparison.

From operator S2, we can have the process $SS^* \rightarrow W^+W^-$. The thermal cross-section is given by [58],

$$\langle \sigma(SS^* \rightarrow W^+W^-) v \rangle = \frac{4}{\pi} \frac{m_S^2}{\Lambda_{S2}^4} \sqrt{1 - \frac{m_W^2}{m_S^2}} \left(1 - \frac{m_W^2}{m_S^2} + \frac{3}{8} \frac{m_W^4}{m_S^4} \right) \quad (5.1)$$

Dark Matter Effective Operators vs Continuum Spectrum Processes		
S1	$\frac{1}{\Lambda_{S1}^2} SS^* B_{\mu\nu} B^{\mu\nu}$	None
S2	$\frac{1}{\Lambda_{S2}^2} SS^* W_{\mu\nu}^a W^{a\mu\nu}$	W^+W^-
F	$\frac{1}{\Lambda_F} \bar{\chi} \gamma^{\mu\nu} \chi B_{\mu\nu}$	W^+W^-, f^+f^-

Table 3: Dark matter effective operators for continuum spectrum signals. The S1 operator does not generate any *continuum spectrum final states* we have considered here. The S2 operator generates only W^+W^- final states, and the fermionic dark matter, F operator, annihilates to both W^+W^- and f^+f^- , with f standing for any electrically charged SM fermion [58].

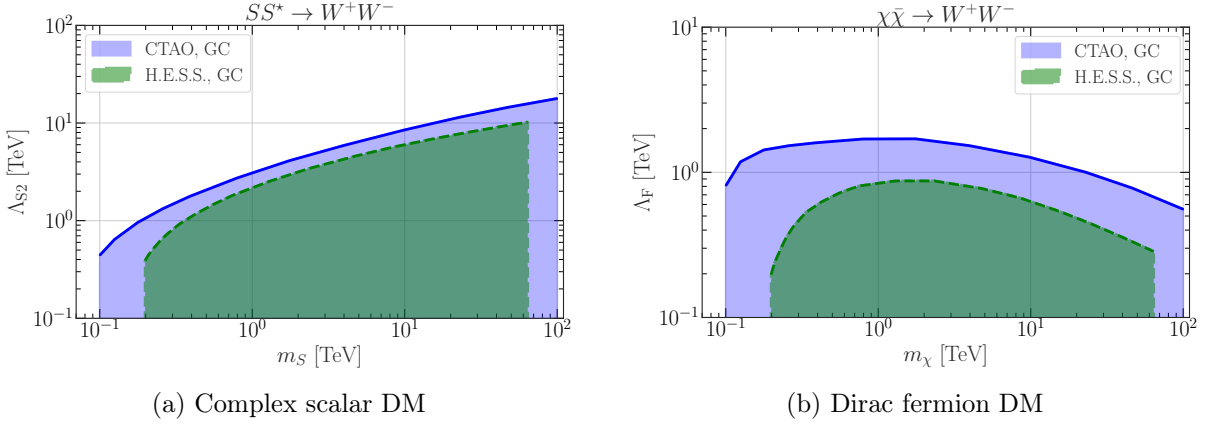


Figure 3: CTAO (solid blue region) and H.E.S.S. (dashed green region) upper limits on the effective energy scales for the diffuse gamma-rays from $X\bar{X} \rightarrow W^+W^-$ annihilation process. We highlight that the CTAO and H.E.S.S. limits come from GC observations using an Einasto density profile [34, 56].

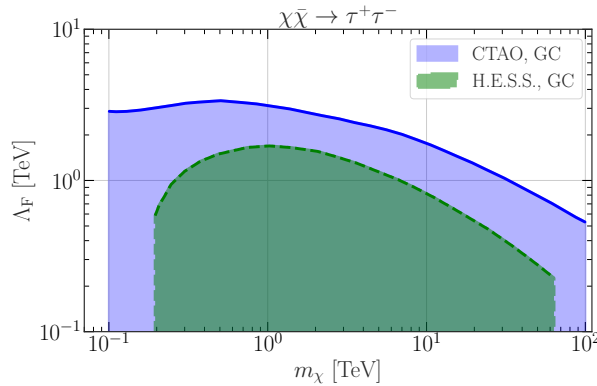


Figure 4: CTAO (solid blue) and H.E.S.S. (dashed green) upper limits on the effective energy scales for the diffuse gamma-rays from $X\bar{X} \rightarrow \tau^+\tau^-$ annihilation process at GC assuming an Einasto density profile.

where $m_W = 80.377$ GeV is W boson mass, and $v_{SM} = 246.22$ GeV is the vacuum expectation value of the SM Higgs field. From operator F directly induces annihilation into all electrically charged pairs of SM particles, but we choose the W^+W^- and $\tau^+\tau^-$ channels for exemplification.

The corresponding annihilation cross-sections are given by [58],

$$\begin{aligned} \langle \sigma(\chi\bar{\chi} \rightarrow W^+W^-) v \rangle &= \frac{1}{4\pi} \frac{m_Z^2 \sin^2 \theta_W}{v_{\text{SM}}^2 \Lambda_{\text{F}}^2} \left(1 - \frac{m_Z^2}{4m_\chi^2}\right)^{-2} \left(1 - \frac{m_W^2}{m_\chi^2}\right)^{3/2} \\ &\times \left(1 + \frac{23}{4} \frac{m_W^2}{m_\chi^2} + \frac{3}{4} \frac{m_W^4}{m_\chi^4}\right), \end{aligned} \quad (5.2)$$

$$\langle \sigma(\chi\bar{\chi} \rightarrow \tau^+\tau^-) v \rangle = \frac{1}{4\pi} \sqrt{1 - \frac{m_\tau^2}{m_\chi^2}} \frac{m_Z^2 \sin^2 \theta_W}{v_{\text{SM}}^2 \Lambda_{\text{F}}^2} \left(1 - \frac{m_Z^2}{4m_\chi^2}\right)^{-2} \quad (5.3)$$

$$\times \left[4\mathcal{A}_\tau^2 + \left(\frac{m_\tau}{m_\chi}\right)^2 (2\mathcal{A}_\tau^2 - 1) + 1\right], \quad (5.4)$$

where $\mathcal{A}_\tau = 2Q_\tau (1 - m_Z^2/m_\chi^2) + 1/2$, and m_τ and Q_τ are the τ mass and electric charge (in natural units). Tab. 3 summarizes the *continuum spectrum charged final states* for each effective operator.

We show the CTAO and H.E.S.S. limits for each final state in Figures 3 and 4. The blue region represents the expected CTAO upper limit for GC. Thus, for both scalar and fermion dark matter CTAO will greatly improve existing limits, reaching effective energy scales above 1 TeV depending on the dark matter mass and final state.

It was important to do this exercise because our effective operators also induce a continuous gamma-ray spectrum. Hence, it is clear that CTAO will surpass its predecessors in the detection of a diffuse component gamma-ray component and line emission, as we will address later.

5.2 Direct detection

In addition to the existing bounds from the continuum spectrum, we extend the analysis to discuss the approximate direct detection limits on the effective energy scales for the Dirac fermion DM. The operator F can describe the interaction of the Dirac dark matter with photons via an anomalous magnetic dipole moment μ_χ [59, 60],

$$\mathcal{L}_\chi = -\frac{\mu_\chi}{2} \bar{\chi} \gamma^{\mu\nu} \chi F_{\mu\nu}, \quad (5.5)$$

where $F_{\mu\nu}$ is the electromagnetic field-strength tensor. The interaction between nucleons and photons comes from the SM neutral current Lagrangian,

$$\mathcal{L}_{\text{NC}} \supset -e J_{\text{EM}}^\mu A_\mu, \quad (5.6)$$

where e is the electric charge and $J_{\text{EM}}^\mu = \bar{\psi}_q \gamma^\mu \psi_q$, for quarks ψ_q . In the non-relativistic limit, the DM-nucleus differential scattering cross-section is given by, [60, 61]

$$\begin{aligned} \frac{d\sigma_{\text{T}}}{dE_{\text{R}}} &= \frac{e^2 \mu_\chi^2}{8\pi} \frac{m_{\text{T}}}{m_{\text{N}}^2} \frac{1}{v^2} \left[2 \frac{m_{\text{N}}^2}{m_{\text{T}}} \left(\frac{v^2}{E_{\text{R}}} - \frac{m_\chi + 2m_{\text{T}}}{2m_\chi m_{\text{T}}} \right) F_{\text{M}}^{p,p}(q^2) + 4F_{\Delta}^{p,p}(q^2) \right. \\ &\quad \left. - 2 \sum_{\text{N}} g_{\text{N}} F_{\Sigma'\Delta}^{\text{N},\text{N}'}(q^2) + \frac{1}{4} \sum_{\text{N},\text{N}'} g_{\text{N}} g_{\text{N}'} F_{\Sigma'}^{\text{N},\text{N}'}(q^2) \right], \end{aligned} \quad (5.7)$$

where E_{R} (expressed in keV) and $q^2 = 2m_{\text{T}}E_{\text{R}}$ are the nuclear recoil energy and the recoil momentum, respectively. The relative velocity is v , m_{T} denotes the target nucleus mass, and for $N = p, n$, Q_{N} are the nucleon electric charges ($Q_p = 1, Q_n = 0$) and g_{N} are the nucleon g -factors ($g_p = 5.59, g_n = -3.83$). Moreover, $F_X^{\text{N},\text{N}'}$ are nuclear form factors, where $X = \text{M}, \Delta, \Sigma'\Delta, \Sigma'$ encompasses different nucleon properties in the target nucleus T [61]. The DM-nucleus differential scattering cross-section above has both spin-dependent (SD) and spin-independent (SI) interaction terms because the dark matter magnetic moment couples to the nuclear magnetic

moment and coherently to the nuclear charge current in the dark matter rest frame, respectively [59]. Looking at the equation, the F_M gives the standard SI cross-section and the standard SD is a combination of $F_{\Sigma'}$ and $F_{\Sigma''}$, in which the last one does not appear here. The reader may find richer details in [51].

Since the SD and SI interactions are tightly connected, we cannot simply compare our theoretical results against the standard SI or SD limits reported by the XENON or LUX-ZEPLIN collaborations. Therefore, we constrain the theoretical number of events predicted by the model operator, which can be determined from the differential scattering cross-section via the differential recoil rate with a given target T,

$$\frac{dR_T}{dE_R} = \frac{\rho_\chi}{m_\chi m_T} \int_{v>v_{\min}} v f(v) \frac{d\sigma_T}{dE_R} dv, \quad (5.8)$$

where the dark matter density is ρ_χ , $v_{\min} = \sqrt{m_T E_R / (2\mu_{\chi,T}^2)}$, with $\mu_{\chi,T} = m_\chi m_T / (m_\chi + m_T)$ denoting the reduced mass, and $f(v)$ is the usual Maxwell-Boltzmann dark matter velocity distribution. Essentially, after integrating over the nuclear recoil energy taking into account the detector's efficiency, the total number of events predicted by the theory in a single energy bin is given by [62, 63]

$$N = \omega R, \quad (5.9)$$

where ω is exposure (kg·days) and R is the total event rate of DM scattering on nucleus ($\text{kg}^{-1} \cdot \text{days}^{-1}$). These calculations were done in Mathematica by combining the `DirectDM` and the `DMFormFactor` software packages [51, 64–68]. The former computed the match of Wilson coefficients of our model onto the non-relativistic EFT at nuclear scale. The latter was used to obtain the theoretical number of events because it calculates the total event rate. The total number of events was obtained from the numerical integration of the event rate and detector efficiency over the possible nuclear recoil energy. We took the efficiency curves reported by XENON1T, XENONnT, and LUX-ZEPLIN experiments [2, 3, 69]. We show the approximate limits for each experiment in Fig. 5. The dotted orange, dashed red, and solid magenta curves are the XENON1T, XENONnT, and LUX-ZEPLIN limits that exclude the parameter space region below the curves.

6 Results

Using the Alpha configuration, the CTAO has derived expected upper limits on the dark matter annihilation cross-section into gamma-ray lines at 95% confidence level (C.L.) for two astrophysical targets, the GC and dSphs [9]. We have written effective operators for scalar and fermion dark matter particles that represent dark matter annihilation into gamma-ray lines. The dark matter annihilation cross-sections depend on the effective energy scale and dark matter mass. With this information, we can use CTAO expected limits to produce expected bounds on the effective energy scale as a function of the dark matter masses m_X for each astrophysical target.

These results are summarized in Fig. 5. The solid pink and dashed green curves represent the lower limits for GC and dSphs, respectively, as the thermally averaged annihilation cross-section is inversely proportional to the energy scale. Since the J -factor of the GC target is much higher than that of dSphs, which increases the probability of a dark matter signal, the GC places stronger limits on the effective energy scales than the dSphs. As expected, the dSphs are less stringent but more solid because are subject to smaller astrophysical uncertainties.

Stronger experimental limits on the dark matter annihilation cross-section translate into more stringent lower bounds on the new physics effective scale. Consequently, operators predicting larger annihilation rates are more tightly constrained. This explains why operators for fermionic dark matter are more restricted than those for scalar dark matter. Similarly, the

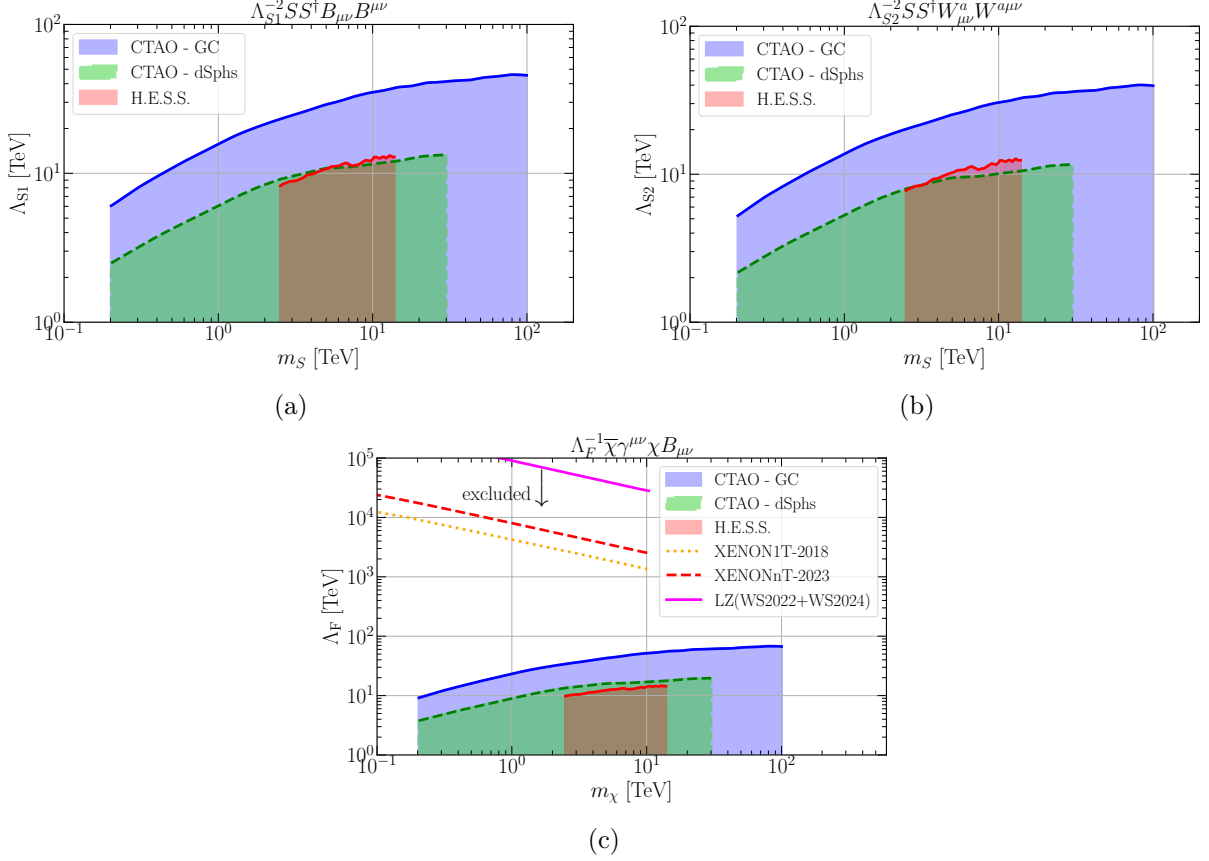


Figure 5: The projected lower limits on the effective energy scales as a function of the dark matter mass based on gamma-ray observations of the GC (blue) and dSphs (green). The magenta solid (LUX-ZEPLIN), read dashed (XENONnT), and orange dotted curves (XENON1T) delimit the correct exclusion limits from direct detection experiments.

operator coupling scalar dark matter to the hypercharge field strength, $SS^\dagger B_{\mu\nu} B^{\mu\nu}$, is more constrained than the operator for the weak gauge fields, $SS^\dagger W_{\mu\nu}^a W^{a\mu\nu}$, due to the difference in coupling strengths.

We observe that the CTAO is expected to probe effective scales well beyond current limits. For dark matter in the TeV mass range, projections indicate CTAO can probe $\Lambda > 10$ TeV for both scalar and fermionic candidates. The sensitivity is particularly impressive for fermionic DM, where CTAO could reach scales of $\Lambda \sim 60$ TeV for $m_\chi = 100$ TeV. Moreover, it is clear that observations from dSphs are less stringent overall.

In Fig. 5, we also exhibit the current limits from H.E.S.S telescope on gamma-ray lines from dark matter annihilation, adopting an Einasto density profile [43]. H.E.S.S. searched for a monoenergetic spectral line from dark matter annihilation in the 300 GeV – 70 TeV energy range during 10 years (254h live time) [7]. Notably, the CTAO expected sensitivity is a factor of a few better. One should bear in mind that as the annihilation cross section is proportional to $1/\Lambda^4$, thus in the $\Lambda - mass$ plane, the difference in sensitivity between the instruments is not much perceived. In terms of annihilation cross section, CTAO is expected to improve H.E.S.S. bounds by an order of magnitude for a dark matter mass of 10 TeV.

Regarding direct direction, the first two operators yield no signal, but the fermion operator does, in the form of a magnetic dipole moment. For this reason, we display the current limits from XENON1T (dotted orange), XENONnT (dashed red), and LUX-ZEPLIN (solid magenta). They are orders of magnitude stronger than those rising from any gamma-ray instrument. We point out that this conclusion is a direct consequence of the presence of a $B_{\mu\nu}$ term. Although

GC	$\Lambda_{S1}^{-2} SS^* B_{\mu\nu} B^{\mu\nu}$	$\Lambda_{S2}^{-2} SS^* W_{\mu\nu}^a W^{a\mu\nu}$	$\Lambda_F^{-1} \bar{\chi} \gamma^{\mu\nu} \chi B_{\mu\nu}$
m_X [TeV]	Λ_{\min} [TeV]	Λ_{\min} [TeV]	Λ_{\min} [TeV]
1	15.75	13.61	23.23
10	35.19	30.52	51.62
100	45.65	39.73	67.11

dSphs	$\Lambda_{S1}^{-2} SS^* B_{\mu\nu} B^{\mu\nu}$	$\Lambda_{S2}^{-2} SS^* W_{\mu\nu}^a W^{a\mu\nu}$	$\Lambda_F^{-1} \bar{\chi} \gamma^{\mu\nu} \chi B_{\mu\nu}$
m_X [TeV]	Λ_{\min} [TeV]	Λ_{\min} [TeV]	Λ_{\min} [TeV]
0.2	2.47	2.13	3.75
1	6.03	5.26	8.94
10	11.59	10.06	17.01

Table 4: CTAO projected lower bounds on the effective energy scales $\Lambda_{\mathcal{O}}$ ($\mathcal{O} = S1, S2, F$) as a function of the dark matter masses m_X ($X = S, \chi$) from gamma-ray lines coming from the GC and dSphs.

both constraints consider the same magnetic dipole moment operator, the annihilation cross-section features higher powers of the field strength tensor to get the $\gamma\gamma$ or γZ final states, and then, it scales as $1/\Lambda_F^4$. Instead, the DM-nucleus differential scattering cross-section (and so the event rate) goes as $1/\Lambda_F^2$. Hence, one does not need to go to higher orders to get the relevant contribution to such scattering. Anyway, we solidly conclude that CTAO will probe effective energy scales above 10 TeV and constitute a powerful dark matter probe for gamma-ray lines.

We summarize the lower limits on the effective energy scales for benchmark points of m_X for each astrophysical target in Tab. 4. For completeness, we use these lower limits to plot the averaged annihilation cross-sections, from Sect. 4, as a function of the dark matter mass in Figs. 6 and 7 for the GC and the dSphs targets, respectively. The arrangement of different sub-figures is similar: the panels (a) and (b) show the scalar dark matter annihilating into $\gamma\gamma$ and γZ lines through the S1 and S2 operators, respectively, with panel (c) showing the fermion dark matter annihilating into the same final states but for the fermionic operators. The colors of the curves stand for different energy scales, while the dotted and solid styles represent the $\gamma\gamma$ and γZ final states, respectively.

7 Conclusions

The construction of the CTAO represents a significant advancement in our quest to comprehend the fundamental nature of dark matter. It will surpass previous gamma-ray telescopes in many ways, and probe gamma-ray photons over several decades in energy, going from 20 GeV to 300 TeV. Besides this broad energy coverage, the energy resolution is a key characteristic of this instrument, enabling the identification of distinct features in gamma-ray spectra associated with line signals. Having in mind that gamma-ray lines are smoking-gun signatures of dark matter annihilation and the exquisite energy resolution of CTAO at TeV energies, we assess CTAO sensitivity to scalar and fermionic dark matter using effective field theory.

We describe dark matter annihilations into gamma-ray lines using dimension five and six effective operators and compare the expected gamma-ray signals with the projected CTAO sensitivity to gamma-ray lines stemming from the Galactic Centre and Dwarf Spheroidal Galaxies to derive projected bounds on the effective energy scale.

Considering the emission of both $\gamma\gamma$ and γZ lines, our results indicate that CTAO will be able to probe effective energy scales up to 67 TeV from gamma-ray observations of the Galactic Centre, with Dwarf Spheroidal Galaxies offering much less sensitive limits. We put our findings

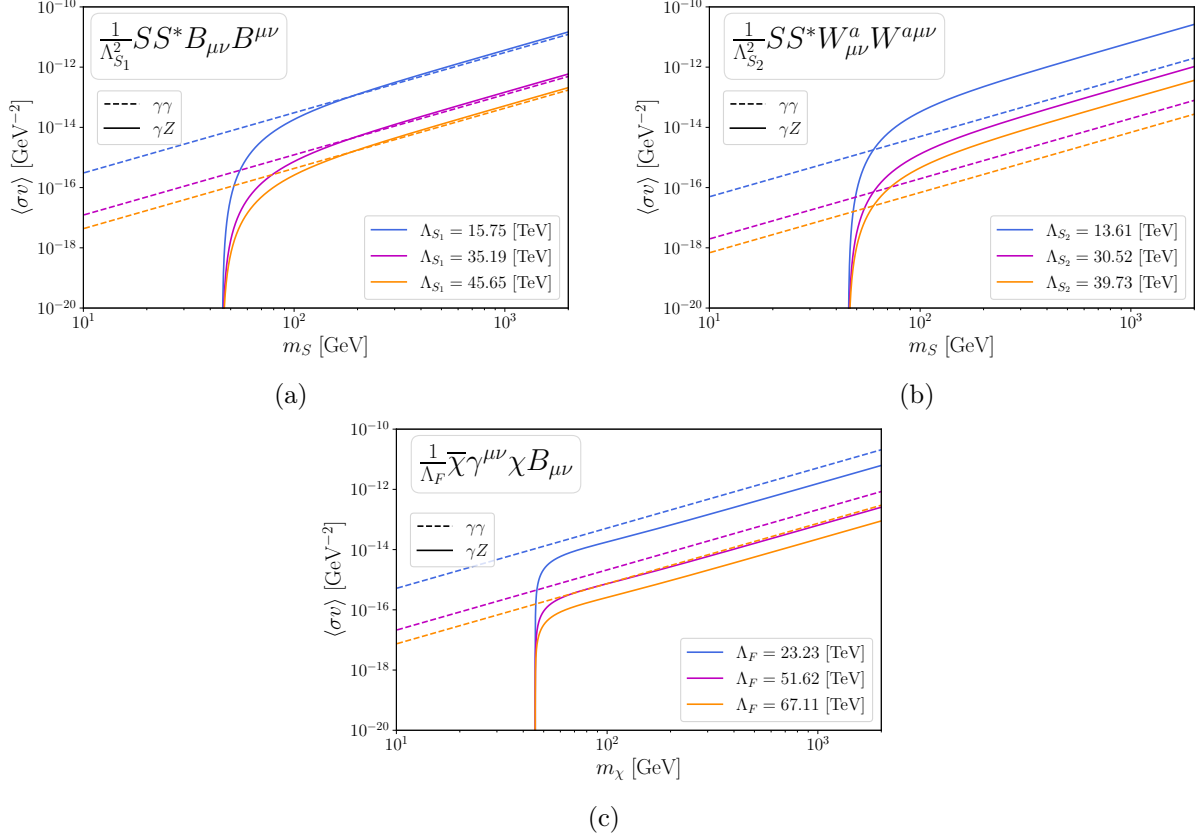


Figure 6: Galactic Centre: thermally averaged annihilation cross-section as a function of the scalar S and fermion χ dark matter masses. Dark matter annihilates into $\gamma\gamma$ (dotted lines) and γZ (solid lines) final states for different energy scales Λ , indicated by the colors.

into perspective with direct detection data, and found that direct detection experiments can be orders of magnitude more constraining than gamma-ray instruments for the dimension five operator involving a fermion dark matter field. For the effective operators involving a scalar field, we conclude that CTAO will constitute a discovery route.

Our conclusions rely on the lowest-order effective operators for scalar and fermion dark matter. Either way, CTAO will set new standards in the dark matter siege.

Acknowledgments

The authors thank Guillermo Gambini, Giorgio Arcadi, Juan Carlos, Tessio Melo, Sergey Kovalenko, Juri Smirnov, and José R. Alves for insightful discussions. Furthermore, the authors thank Clarissa Siqueira, Martin White, and Ruoyu Shang for their relevant internal peer review of the manuscript within the CTAO collaboration. The authors acknowledge the National Laboratory for Scientific Computing (LNCC/MCTI, Brazil) for providing HPC resources of the SDumont supercomputer (<http://sdumont.lncc.br>). The authors acknowledge the use of the International Institute of Physics (IIP) cluster “bulletcluster”. This work was supported by Simons Foundation (Award Number:1023171-RC), 1699/24 IIF-FINEP, FAPESP Grant 2018/25225-9, 2021/01089-1, 2023/01197-4, ICTP-SAIFR FAPESP Grants 2021/14335-0, CNPq Grant 307130/2021-5, CNPq Grant 200513/2025-7, and ANID-Millennium Science Initiative Program CN2019_044. LA acknowledges the support from Coordenação de Aperfeiçoamento de Pessoal de Nível Superior (CAPES) under grant 88887.827404/2023-00. The work of D.B. is supported by the Science and Engineering Research Board (SERB), Government of India grants MTR/2022/000575 and CRG/2022/000603. D.B. also acknowledges the

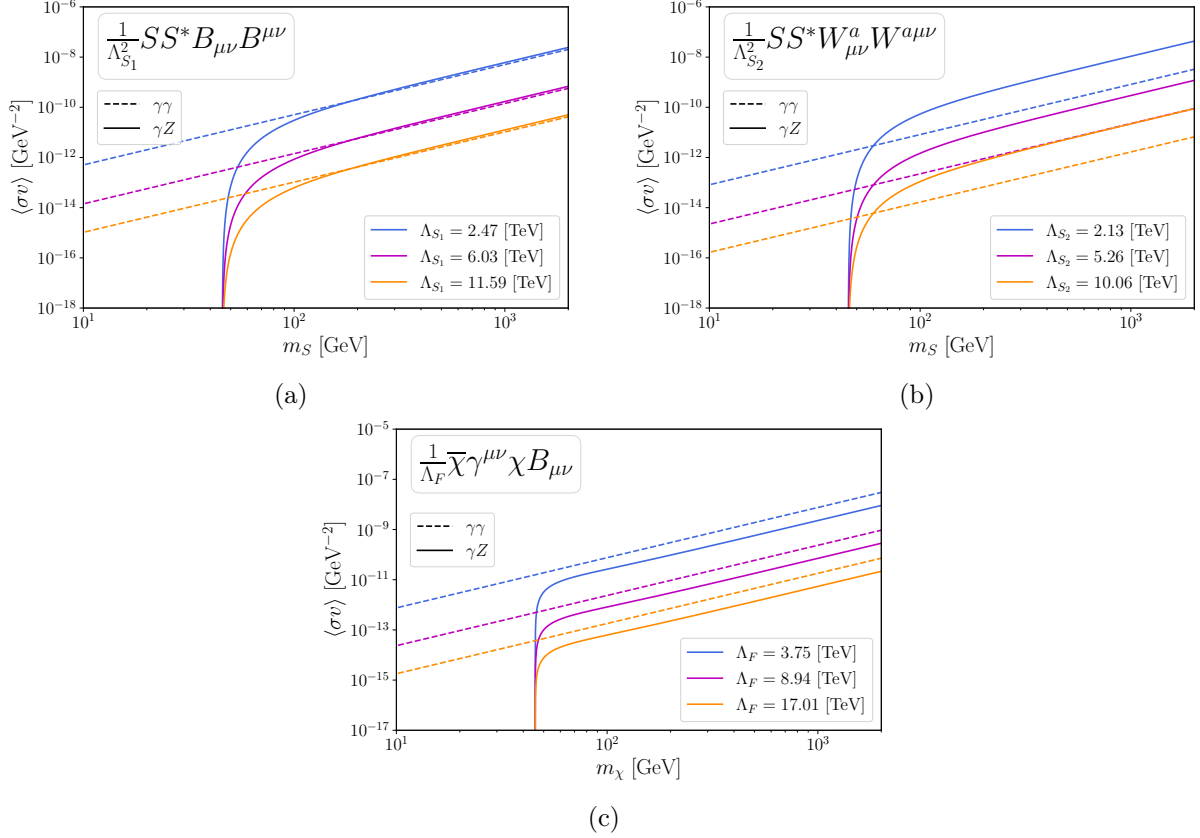


Figure 7: Dwarf Spheroidal Galaxies: thermally averaged annihilation cross-section as a function of the scalar S and fermion χ dark matter masses for annihilation into $\gamma\gamma$ (dotted lines) and γZ (solid lines) lines for different energy scales Λ indicated by the colors.

support from the Fulbright-Nehru Academic and Professional Excellence Award 2024-25. JPN acknowledges support from the Programa Institucional de Internacionalização (PrInt) and the Coordenação de Aperfeiçoamento de Pessoal de Nível Superior (CAPES) under the CAPES-PrInt Grant No. 88887.912033/2023-00. JPN is grateful to the Mainz Institute for Theoretical Physics (MITP) of the Cluster of Excellence PRISMA+ (Project ID 390831469) for its hospitality and partial support during the initial stages of this work. JPN thanks the University of Liverpool for the hospitality during the final stages of this project.

References

- [1] **Planck** Collaboration, N. Aghanim *et. al.*, *Planck 2018 results. VI. Cosmological parameters*, *Astron. Astrophys.* **641** (2020) A6, [[1807.06209](#)]. [Erratum: *Astron.Astrophys.* 652, C4 (2021)].
- [2] **LZ Collaboration** Collaboration, J. Aalbers *et. al.*, *Dark Matter Search Results from 4.2 Tonne-Years of Exposure of the LUX-ZEPLIN (LZ) Experiment*, [[2410.17036](#)].
- [3] **XENON** Collaboration, E. Aprile *et. al.*, *First Dark Matter Search with Nuclear Recoils from the XENONnT Experiment*, *Phys. Rev. Lett.* **131** (2023), no. 4 041003, [[2303.14729](#)].
- [4] **ATLAS** Collaboration, G. Aad *et. al.*, *Constraints on dark matter models involving an s-channel mediator with the ATLAS detector in pp collisions at $\sqrt{s} = 13$ TeV*, [[2404.15930](#)].
- [5] **CMS** Collaboration, A. Hayrapetyan *et. al.*, *Dark sector searches with the CMS experiment*, [[2405.13778](#)].
- [6] **Fermi-LAT** Collaboration, M. Ackermann *et. al.*, *Updated search for spectral lines from Galactic dark matter interactions with pass 8 data from the Fermi Large Area Telescope*, *Phys. Rev. D* **91** (2015), no. 12 122002, [[1506.00013](#)].

- [7] **HESS** Collaboration, H. Abdallah *et. al.*, *Search for γ -Ray Line Signals from Dark Matter Annihilations in the Inner Galactic Halo from 10 Years of Observations with H.E.S.S.*, *Phys. Rev. Lett.* **120** (2018), no. 20 201101, [[1805.05741](#)].
- [8] J. W. Foster, Y. Park, B. R. Safdi, Y. Soreq, and W. L. Xu, *Search for dark matter lines at the Galactic Center with 14 years of Fermi data*, *Phys. Rev. D* **107** (2023), no. 10 103047, [[2212.07435](#)].
- [9] **CTAO** Collaboration, S. Abe *et. al.*, *Dark matter line searches with the Cherenkov Telescope Array*, *JCAP* **07** (2024) 047, [[2403.04857](#)].
- [10] T. Bringmann and C. Weniger, *Gamma Ray Signals from Dark Matter: Concepts, Status and Prospects*, *Phys. Dark Univ.* **1** (2012) 194–217, [[1208.5481](#)].
- [11] J. M. Gaskins, *A review of indirect searches for particle dark matter*, *Contemp. Phys.* **57** (2016), no. 4 496–525, [[1604.00014](#)].
- [12] C. Pérez de los Heros, *Status, Challenges and Directions in Indirect Dark Matter Searches*, *Symmetry* **12** (2020), no. 10 1648, [[2008.11561](#)].
- [13] K. N. Abazajian, S. Blanchet, and J. P. Harding, *Current and Future Constraints on Dark Matter from Prompt and Inverse-Compton Photon Emission in the Isotropic Diffuse Gamma-ray Background*, *Phys. Rev. D* **85** (2012) 043509, [[1011.5090](#)].
- [14] K. N. Abazajian, P. Agrawal, Z. Chacko, and C. Kilic, *Conservative Constraints on Dark Matter from the Fermi-LAT Isotropic Diffuse Gamma-Ray Background Spectrum*, *JCAP* **11** (2010) 041, [[1002.3820](#)].
- [15] T. Bringmann, F. Calore, G. Vertongen, and C. Weniger, *On the Relevance of Sharp Gamma-Ray Features for Indirect Dark Matter Searches*, *Phys. Rev. D* **84** (2011) 103525, [[1106.1874](#)].
- [16] K. N. Abazajian, P. Agrawal, Z. Chacko, and C. Kilic, *Lower Limits on the Strengths of Gamma Ray Lines from WIMP Dark Matter Annihilation*, *Phys. Rev. D* **85** (2012) 123543, [[1111.2835](#)].
- [17] K. N. Abazajian and J. P. Harding, *Constraints on WIMP and Sommerfeld-Enhanced Dark Matter Annihilation from HESS Observations of the Galactic Center*, *JCAP* **01** (2012) 041, [[1110.6151](#)].
- [18] **Fermi-LAT** Collaboration, M. Ackermann *et. al.*, *Searching for Dark Matter Annihilation from Milky Way Dwarf Spheroidal Galaxies with Six Years of Fermi Large Area Telescope Data*, *Phys. Rev. Lett.* **115** (2015), no. 23 231301, [[1503.02641](#)].
- [19] M. G. Baring, T. Ghosh, F. S. Queiroz, and K. Sinha, *New Limits on the Dark Matter Lifetime from Dwarf Spheroidal Galaxies using Fermi-LAT*, *Phys. Rev. D* **93** (2016), no. 10 103009, [[1510.00389](#)].
- [20] C. Garcia-Cely and A. Ibarra, *Novel Gamma-ray Spectral Features in the Inert Doublet Model*, *JCAP* **09** (2013) 025, [[1306.4681](#)].
- [21] F. S. Queiroz, C. E. Yaguna, and C. Weniger, *Gamma-ray Limits on Neutrino Lines*, *JCAP* **05** (2016) 050, [[1602.05966](#)].
- [22] S. Profumo, F. S. Queiroz, and C. E. Yaguna, *Extending Fermi-LAT and H.E.S.S. Limits on Gamma-ray Lines from Dark Matter Annihilation*, *Mon. Not. Roy. Astron. Soc.* **461** (2016), no. 4 3976–3981, [[1602.08501](#)].
- [23] **H.E.S.S.** Collaboration, H. Abdallah *et. al.*, *Search for dark matter annihilations towards the inner Galactic halo from 10 years of observations with H.E.S.S.*, *Phys. Rev. Lett.* **117** (2016), no. 11 111301, [[1607.08142](#)].
- [24] S. Profumo, F. S. Queiroz, J. Silk, and C. Siqueira, *Searching for Secluded Dark Matter with H.E.S.S., Fermi-LAT, and Planck*, *JCAP* **03** (2018) 010, [[1711.03133](#)].
- [25] F. S. Queiroz and C. Siqueira, *Search for Semi-Annihilating Dark Matter with Fermi-LAT, H.E.S.S., Planck, and the Cherenkov Telescope Array*, *JCAP* **04** (2019) 048, [[1901.10494](#)].
- [26] K. N. Abazajian, S. Horiuchi, M. Kaplinghat, R. E. Keeley, and O. Macias, *Strong constraints on thermal relic dark matter from Fermi-LAT observations of the Galactic Center*, *Phys. Rev. D* **102** (2020), no. 4 043012, [[2003.10416](#)].

- [27] C. Siqueira, G. N. Fortes, A. Viana, and F. S. Queiroz, *Indirect Searches for Secluded Dark Matter*, *PoS ICRC2021* (2021) 577, [[2107.04053](#)].
- [28] D. Bose, V. R. Chitnis, P. Majumdar, and A. Shukla, *Galactic and extragalactic sources of very high energy gamma rays*, *Eur. Phys. J. ST* **231** (2022), no. 1 27–66, [[2201.06789](#)].
- [29] G. Arcadi, D. Cabo-Almeida, M. Dutra, P. Ghosh, M. Lindner, Y. Mambrini, J. P. Neto, M. Pierre, S. Profumo, and F. S. Queiroz, *The Waning of the WIMP: Endgame?*, [2403.15860](#).
- [30] C. Collaboration, *CTAO Performance*, 2025.
<https://www.ctao.org/for-scientists/performance/> (last access: 2025-09-07).
- [31] A. Ibarra, H. M. Lee, S. López Gehler, W.-I. Park, and M. Pato, *Gamma-ray boxes from axion-mediated dark matter*, *JCAP* **05** (2013) 016, [[1303.6632](#)]. [Erratum: *JCAP* **03**, E01 (2016)].
- [32] A. Ibarra, A. S. Lamperstorfer, S. López-Gehler, M. Pato, and G. Bertone, *On the sensitivity of CTA to gamma-ray boxes from multi-TeV dark matter*, *JCAP* **09** (2015) 048, [[1503.06797](#)]. [Erratum: *JCAP* **06**, E02 (2016)].
- [33] T. Bringmann, L. Bergstrom, and J. Edsjo, *New Gamma-Ray Contributions to Supersymmetric Dark Matter Annihilation*, *JHEP* **01** (2008) 049, [[0710.3169](#)].
- [34] CTA Collaboration, A. Acharyya *et. al.*, *Sensitivity of the Cherenkov Telescope Array to a dark matter signal from the Galactic centre*, *JCAP* **01** (2021) 057, [[2007.16129](#)].
- [35] P. Panci, *Electroweak Multiplets as Dark Matter candidates: A brief review*, 5, 2024. [2405.05087](#).
- [36] C. Dubos, P. Sharma, S. Patel, and T. Suomijärvi, *Cherenkov Telescope Array Observatory sensitivity to heavy Galactic Cosmic Rays and the shape of particle spectrum*, *JCAP* **02** (2025) 078, [[2410.21199](#)].
- [37] T. Hassan, L. Arrabito, K. Bernlöhner, J. Bregeon, J. Cortina, P. Cumani, F. Di Pierro, D. Falceta-Goncalves, R. G. Lang, J. Hinton, T. Jogler, G. Maier, A. Moralejo, A. Morselli, C. J. Todero Peixoto, and M. Wood, *Monte Carlo performance studies for the site selection of the Cherenkov Telescope Array*, *Astroparticle Physics* **93** (July, 2017) 76–85, [[1705.01790](#)].
- [38] D. G. Cerdeno, M. Peiro, and S. Robles, *Enhanced lines and box-shaped features in the gamma-ray spectrum from annihilating dark matter in the NMSSM*, *JCAP* **04** (2016) 011, [[1507.08974](#)].
- [39] M. Duerr, P. Fileviez Perez, and J. Smirnov, *Simplified Dirac Dark Matter Models and Gamma-Ray Lines*, *Phys. Rev. D* **92** (2015), no. 8 083521, [[1506.05107](#)].
- [40] K. K. Boddy, K. R. Dienes, D. Kim, J. Kumar, J.-C. Park, and B. Thomas, *Lines and Boxes: Unmasking Dynamical Dark Matter through Correlations in the MeV Gamma-Ray Spectrum*, *Phys. Rev. D* **94** (2016), no. 9 095027, [[1606.07440](#)].
- [41] F. S. Queiroz and C. E. Yaguna, *Gamma-ray lines may reveal the CP nature of the dark matter particle*, *JCAP* **01** (2019) 047, [[1810.07068](#)].
- [42] K.-C. Yang, *A potentially detectable gamma-ray line in the Fermi Galactic center excess — in light of one-step cascade annihilations of secluded (vector) dark matter via the Higgs portal*, *JHEP* **07** (2020) 148, [[2001.04946](#)].
- [43] L. Angel, G. Gambini, L. Guedes, F. S. Queiroz, and V. de Souza, *Constraining gamma-ray lines from dark matter annihilation using Fermi-LAT and H.E.S.S. data*, *JCAP* **04** (2024) 028, [[2311.17827](#)].
- [44] P. De La Torre Luque, J. Smirnov, and T. Linden, *Gamma-ray lines in 15 years of Fermi-LAT data: New constraints on Higgs portal dark matter*, *Phys. Rev. D* **109** (2024), no. 4 L041301, [[2309.03281](#)].
- [45] J.-G. Cheng, Y.-F. Liang, and E.-W. Liang, *Search for the gamma-ray spectral lines with the DAMPE and the Fermi-LAT observations*, *Phys. Rev. D* **108** (2023), no. 6 063015, [[2308.16762](#)].
- [46] M. Cirelli, A. Strumia, and J. Zupan, *Dark Matter*, [2406.01705](#).
- [47] M. Beltran, D. Hooper, E. W. Kolb, and Z. C. Krusberg, *Deducing the nature of dark matter from direct and indirect detection experiments in the absence of collider signatures of new physics*, *Phys. Rev. D* **80** (2009) 043509, [[0808.3384](#)].

- [48] J. Fan, M. Reece, and L.-T. Wang, *Non-relativistic effective theory of dark matter direct detection*, *JCAP* **11** (2010) 042, [[1008.1591](#)].
- [49] J. Goodman, M. Ibe, A. Rajaraman, W. Shepherd, T. M. P. Tait, and H.-B. Yu, *Constraints on Dark Matter from Colliders*, *Phys. Rev. D* **82** (2010) 116010, [[1008.1783](#)].
- [50] M. Beltran, D. Hooper, E. W. Kolb, Z. A. C. Krusberg, and T. M. P. Tait, *Maverick dark matter at colliders*, *JHEP* **09** (2010) 037, [[1002.4137](#)].
- [51] A. L. Fitzpatrick, W. Haxton, E. Katz, N. Lubbers, and Y. Xu, *The Effective Field Theory of Dark Matter Direct Detection*, *JCAP* **02** (2013) 004, [[1203.3542](#)].
- [52] **GAMBIT** Collaboration, P. Athron *et. al.*, *Thermal WIMPs and the scale of new physics: global fits of Dirac dark matter effective field theories*, *Eur. Phys. J. C* **81** (2021), no. 11 992, [[2106.02056](#)].
- [53] S. Bhattacharya and J. Wudka, *Effective theories with dark matter applications*, *Int. J. Mod. Phys. D* **30** (2021), no. 13 2130004, [[2104.01788](#)].
- [54] P. Gondolo and G. Gelmini, *Cosmic abundances of stable particles: Improved analysis*, *Nucl. Phys. B* **360** (1991) 145–179.
- [55] T. R. Slatyer, *Les Houches Lectures on Indirect Detection of Dark Matter*, *SciPost Phys. Lect. Notes* **53** (2022) 1, [[2109.02696](#)].
- [56] **H.E.S.S.** Collaboration, H. Abdalla *et. al.*, *Search for Dark Matter Annihilation Signals in the H.E.S.S. Inner Galaxy Survey*, *Phys. Rev. Lett.* **129** (2022), no. 11 111101, [[2207.10471](#)].
- [57] **Fermi-LAT** Collaboration, M. Ackermann *et. al.*, *The Fermi Galactic Center GeV Excess and Implications for Dark Matter*, *Astrophys. J.* **840** (2017), no. 1 43, [[1704.03910](#)].
- [58] J.-Y. Chen, E. W. Kolb, and L.-T. Wang, *Dark matter coupling to electroweak gauge and Higgs bosons: an effective field theory approach*, *Phys. Dark Univ.* **2** (2013) 200–218, [[1305.0021](#)].
- [59] T. Banks, J.-F. Fortin, and S. Thomas, *Direct Detection of Dark Matter Electromagnetic Dipole Moments*, [[1007.5515](#)].
- [60] E. Del Nobile, *The Theory of Direct Dark Matter Detection: A Guide to Computations*, [[2104.12785](#)].
- [61] B. J. Kavanagh, P. Panci, and R. Ziegler, *Faint Light from Dark Matter: Classifying and Constraining Dark Matter-Photon Effective Operators*, *JHEP* **04** (2019) 089, [[1810.00033](#)].
- [62] D. G. Cerdeno and A. M. Green, *Direct detection of WIMPs*, [[1002.1912](#)].
- [63] M. Cirelli, E. Del Nobile, and P. Panci, *Tools for model-independent bounds in direct dark matter searches*, *JCAP* **10** (2013) 019, [[1307.5955](#)].
- [64] F. Bishara, J. Brod, B. Grinstein, and J. Zupan, *Chiral Effective Theory of Dark Matter Direct Detection*, *JCAP* **02** (2017) 009, [[1611.00368](#)].
- [65] F. Bishara, J. Brod, B. Grinstein, and J. Zupan, *DirectDM: a tool for dark matter direct detection*, [[1708.02678](#)].
- [66] F. Bishara, J. Brod, B. Grinstein, and J. Zupan, *From quarks to nucleons in dark matter direct detection*, *JHEP* **11** (2017) 059, [[1707.06998](#)].
- [67] J. Brod, A. Gootjes-Dreesbach, M. Tamaro, and J. Zupan, *Effective Field Theory for Dark Matter Direct Detection up to Dimension Seven*, *JHEP* **10** (2018) 065, [[1710.10218](#)]. [Erratum: *JHEP* **07**, 012 (2023)].
- [68] N. Anand, A. L. Fitzpatrick, and W. C. Haxton, *Weakly interacting massive particle-nucleus elastic scattering response*, *Phys. Rev. C* **89** (2014), no. 6 065501, [[1308.6288](#)].
- [69] **XENON** Collaboration, E. Aprile *et. al.*, *Dark Matter Search Results from a One Ton-Year Exposure of XENON1T*, *Phys. Rev. Lett.* **121** (2018), no. 11 111302, [[1805.12562](#)].